DOI: 10.1002/ejic.200700732

A New Donor-Stabilized Ditungsten Amido Alkoxido Species: Synthesis, Crystal Structure, Fluxionality, and Grafting onto Silica

Olivier Coutelier,[a] Régis M. Gauvin,*[a] Guy Nowogrocki,[a] Julien Trébosc,[a] Laurent Delevoye,[a] and André Mortreux*[a]

Keywords: Tungsten / Metal-metal multiple bonds / Ligand design / Grafting / Silica / Alkyne metathesis

A new dimeric tungsten(III) complex containing amido and chelating pyridine–alkoxido ligands was synthesized through protonolysis of $[W_2(NMe_2)_6]$ by 2-(2-pyridyl)propan-2-ol and fully characterized by X-ray diffraction and infrared and NMR spectroscopy. Intramolecular exchange processes were studied by variable-temperature NMR spectroscopy. The compound was grafted onto dehydroxylated silica by protonolysis of an amido–tungsten bond, and the structure of the supported species was investigated by infrared and solid-state (bidimensional) NMR spectroscopy. The reactivity of the molecular and grafted species toward alkynes was probed.

Introduction

The recent focus on alkene metathesis following the Nobel prize award to Y. Chauvin, R. R. Schrock, and R. Grubbs has emphasized that the corresponding reaction involving carbon-carbon triple bonds, namely alkyne metathesis,[1] is still a field offering significant challenges.[2] Selectivity of this reaction suffers from side reactions such as trimerization into substituted benzene derivatives, coupling into cyclopentadiene analogues, or polymerization yielding polyacetylenes. The latter reaction is most particularly encountered with terminal alkynes, where the acidity of the terminal C–H induces the rapid formation of polymerization propagating species. Development of new catalysts for this transformation is therefore of considerable interest. Inspired by Schrock's systems based on $[(t\text{BuO})_3W{\equiv}C\text{-}t\text{Bu}]$ and $[(t\text{BuO})_3W{\equiv}W(Ot\text{Bu})_3]$,[3] as well as by our findings on the dramatic influence of quinuclidine as a Lewis base additive in this reaction,[4] we have recently disclosed a new catalytic system that relies on the hemilability concept.[5] Indeed, use of $[W_2(OC(Me)_2CH_2OMe)_6]$ (**2**), in which methoxy donor groups are incorporated within the alkoxido fragments, has led to unprecedented activity for the metathesis of phenylacetylene and 1-heptyne (Scheme 1).[6] The use of alkoxido ligands bearing donor groups thus seems to be a promising approach to develop efficient and selective catalytic systems. In this view, we have chosen to focus on an alkoxido ligand bearing a pyridyl function.[7] Furthermore, Basset and Moore have both reported silica-grafted catalysts displaying high activity and

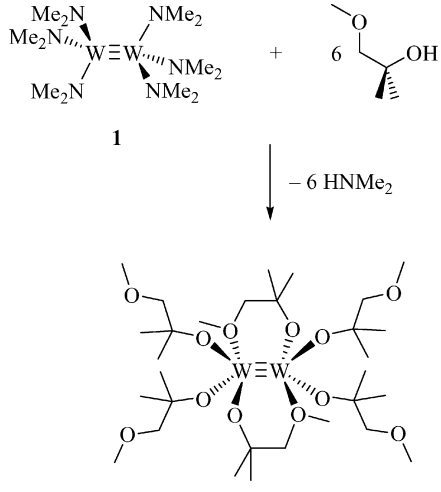

Scheme 1. Synthesis and reactivity of **2**.

[a] Unité de Catalyse et de Chimie du Solide, UMR 8181 CNRS, ENSCL,
B. P. 90108, 59652 Villeneuve d'Ascq Cedex, France
Fax: +33-3-20436585
E-mail: regis.gauvin@ensc-lille.fr
andre.mortreux@ensc-lille.fr
Supporting information for this article is available on the WWW under http://www.eurjic.org or from the author.

selectivity.[8] On the other hand, we have recently shown that the grafting onto silica of compounds inactive as homogeneous catalysts can afford heterogeneous catalysts active toward terminal alkynes.[9] As the supporting of organometallic species plays a significant role in this chemistry, this prompted us to probe the effect of grafting on other (potential) catalysts.

The present contribution describes our results on the synthesis, solid- and liquid-state structural investigations of a ditungsten complex bearing a bidentate pyridylalkoxido ligand, and on its grafting onto dehydroxylated silica to generate binuclear supported species.

Results and Discussion

Synthesis and Characterization of Complex $[W_2(L)_2(NMe_2)_4]$ (3)

The reaction of **1** with 12 equivalents of 2-(2-pyridyl)propan-2-ol, (L)H in toluene at room temperature affords a deep red solution, from which, after stripping off the volatiles and washing with pentane, $[W_2(L)_2(NMe_2)_4]$ (**3**) is obtained as a red-orange solid in 40% yield (Scheme 2). NMR follow-up of the reaction in C_6D_6 in the presence of excess (L)H shows that the reaction does not proceed further, despite extended reaction times and more elevated temperatures. In the presence of six equivalents of (L)H, **1** reacts to afford mainly the monosubstituted complex $[W_2(L)(NMe_2)_5]$, on the basis of ^{1}H NMR spectroscopic data (see electronic supporting information). The addition of six further equivalents of (L)H to the reaction mixture leads to the selective formation of **3** after 12 h. This differs from the reaction of **1** with *tert*-butyl alcohol, which affords under similar conditions the hexakis(alkoxido) dinuclear complex through complete alcoholysis of the dimethylamido ligands. This is most probably due to the strong binding of the chelating pyridine, which prevents coordination of the bulky alcohol, most probably a prerequisite for the protonolysis of the tungsten–amido bond.

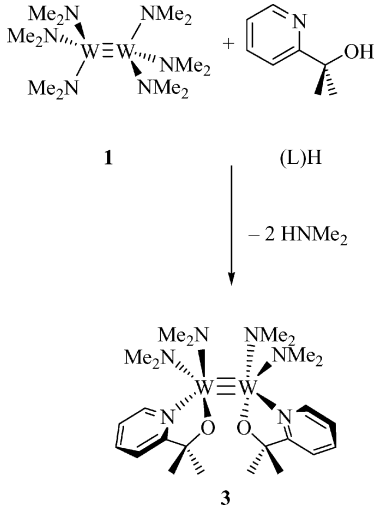

Scheme 2. Synthesis of **3**.

Single crystals suitable for X-ray analysis have been grown in pentane where **3** is slightly soluble. The molecular structure of **3** is depicted in Figure 1. Selected bond lengths and angles are summarized in Table 1.

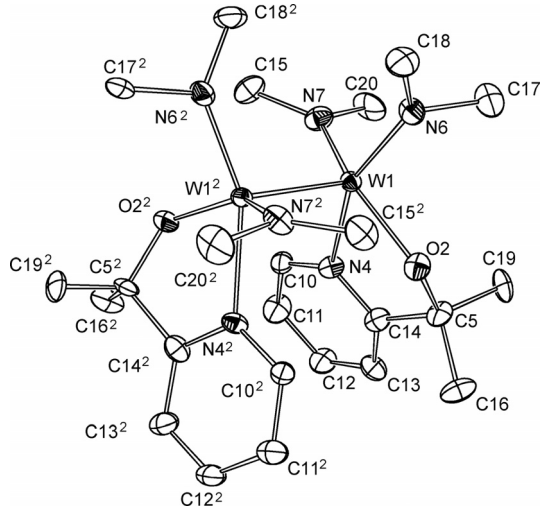

Figure 1. ORTEP representation of **3** with the thermal ellipsoids at 50% of probability. H atoms are omitted for clarity.

Table 1. Selected bond lengths (Å) and angles (°) for complex **3**.

W1–W1²	2.3351(5)	W1–N7	1.986(6)
W1–N4	2.263(5)	W1–N6	1.975(6)
W1–O2	2.021(5)		
N6–W1–N7	101.3(2)	O2–W1–N4	71.63(18)
N6–W1–O2	91.7(3)	N6–W1–W1²	104.05(16)
N7–W1–O2	144.22(19)	N7–W1–W1²	101.79(16)
N6–W1–N4	155.7(2)	O2–W1–W1²	107.14(13)
N7–W1–N4	84.13(19)	N4–W1–W1²	97.81(13)

Each tungsten of the dimer adopts a distorted square-planar coordination [the sum of angles is 348.8(5)°], composed of two dimethylamido and one chelating pyridylalkoxido ligands. The two tungsten-based fragments are connected by a C_2 axis, which intersects the compound at the center of the W–W triple bond. The configuration adopted by the compound is classical for M_2L_8 compounds.[10] The two WL_4 entities are eclipsed, thus minimizing steric repulsions (Figure 2). The bond lengths are classical: the W1–W1² bond length of 2.3351(5) Å is within the expected range[11] {see for example 2.332(1) in $[W_2(OCHMe_2)_6(py)_2]$[12] or 2.3340(5) in $[W_2(OCH_2tBu)_6(py)_2]$[13]}. The pyridine nitrogen to tungsten bond length [2.263(5) Å] is comparable to that observed in similar complexes.[12,13] The tungsten–amido [1.986(6) and 1.975(6) Å] and tungsten–alkoxido [2.021(5) Å] bond lengths are unexceptional. The two nitrogen amido are planar [sum of angles at N6 and N7 of 359.99(9) and 359.35(8)°, respectively], and the NMe_2 fragments are aligned with the W–W triple bond [C18–N6–W1–W1² and C15–N7–W1–W1² dihedral angles of 8.1(7) and 4.5(6)°, respectively]. Thus, proximal methyl groups (C15 and C18) are located over the W–W bond, while distal methyl groups point in the opposite direction.

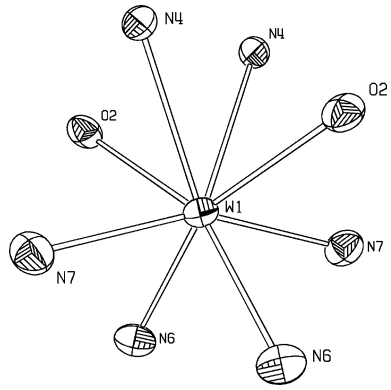

Figure 2. View of the central skeleton of **3** looking down the W1–W1[2] axis.

Room temperature ^{1}H NMR spectroscopic data is consistent with the presence of a single type of [N–O] ligand, indicating that the C_2 symmetry observed in the solid-state is retained in solution. The pyridyl *ortho* C–H gives rise to a characteristic doublet of triplets in the low field region (δ = 9.06 ppm). The two diastereotopic methyl groups resonate at δ = 1.75 and 1.04 ppm. At room temperature, the spectrum comprises three signals for the NMe_2 groups at δ = 4.73, 3.70, and 2.28 ppm, as broad peaks of intensities 6, 12, and 6 H, respectively. This is consistent with two types of NMe_2 groups, and is characteristic of hindered rotation around the W–N bond.[14] In order to shed light on the dynamic processes at hand, variable-temperature NMR studies have been carried out (Figure 3). Two different processes involving the two types of NMe_2 ligands have been observed (Table 2).

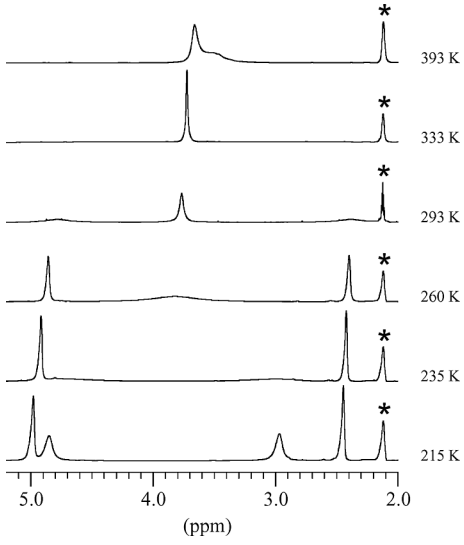

Figure 3. Variable-temperature ^{1}H NMR spectra of complex **3** in the *N*-methyl group region ([D$_8$]toluene, 400 MHz; * denotes solvent peak).

On the basis of the literature data,[16] the shielded and deshielded signals within each of these pairs can be respectively assigned to the distal and proximal methyl groups.

Table 2. Variable-temperature NMR studies on **3**: coalescing pairs of signals and corresponding activation energies ([D$_8$]toluene).

δ [ppm]	T_c [K]	$\Delta G^{\neq}$ [kJ mol^{-1}][15]
4.98, 2.44	333 (±5)	60.4 (±0.1)
4.86, 2.96	245 (±5)	44.4 (±0.1)

This was confirmed by the low-temperature NOESY correlation spectrum, which also allowed us to assign the pairs of signals at δ = 4.98 and 2.44 ppm and at δ = 4.86 and 2.96 ppm to the NMe_2 group in *cis* and *trans* position to the pyridine, respectively, on the basis of interactions with the pyridine *ortho* CH. This is in agreement with the relative energetic barriers: the NMe_2 group *cis* to the pyridine, [$\Delta G^{\neq}$ = 60.4 (±0.1) kJ mol^{-1}] is located in a more congested environment (pyridine and NMe_2 groups) than the *trans* NMe_2 [$\Delta G^{\neq}$ = 44.4 (±0.1) kJ mol^{-1}].

Complex **3** is inactive toward 4-nonyne in the absence of additive. In situ protonolysis with four equivalents of alcohol was attempted to generate $[W_2(OR)_4(L)_2]$ species, bearing in mind the high reactivity of alkoxido species $[W_2(OR)_6]$ in alkyne metathesis. A series of alcohols was screened: *tert*-butyl alcohol, 1-adamantanol, phenol, and 3-quinuclidinol. Only the latter afforded an active catalyst, although a high temperature (363 K) was necessary to reach the thermodynamic equilibrium mixture (1 h). This may be related to this alcohol's coordinative ability through its nitrogen atom. However, further characterization efforts are necessary at this stage to confirm that the amido–tungsten bond protonolysis took place. Moreover, regarding the potential of catalysts bearing this [N,O] ligand in alkyne metathesis, the strongly basic pyridine may hinder the alkyne substrate coordination, a step necessary to cleave the W_2 dimer and generate a catalytically active alkylidine species.

Grafting of Complex 3 Onto Partially Dehydroxylated Silica

These results on the alcoholysis of the W–NMe_2 bond producing a metathesis active system prompted us to study the effect of the grafting of **3** onto an inorganic support, since surface hydroxy groups are frequently compared to ROH moieties.[17] Partially dehydroxylated silica was used as a support for the grafting of **3**. Bearing only isolated silanol groups as protic sites on its surface, silica treated under vacuum at 700 °C behaves as a bulky silanol ligand when reacted with organometallic reagents, affording well-defined single site catalysts.[18] Moreover, metal amido species have been grafted with success onto inorganic supports.[8b,19] More precisely, W–NMe_2 groups readily react with surface silanols to afford covalent ≡Si–O–W bonds, as shown by the studies on the grafting of **1** onto silica.[8] Grafting of **3** onto SiO_2-700 proceeds at room temperature in pentane. During the reaction course, the supernatant color fades from dark to clear orange, while the suspended solid turns to dark red. After three pentane washings and drying at 80 °C for 3 h under a 10^{-6} mbar vacuum, **4** is obtained as an ochre powder (Scheme 3). When carrying out

the reaction between **3** and suspended partially dehydroxylated silica in C_6D_6, the only new compound observed by ^1H NMR was $HNMe_2$. No pyridyl alcohol ligand (L)H was detected, which is consistent with the protonolysis of the W–NMe_2 bond by ≡SiOH as the preferred grafting mode. Elemental analysis indicates a tungsten content of 10.53 wt.-%. The molar ratios N/W and C/W, respectively of 2.46 and 12.23, are close to values expected for ≡Si–O–[$W_2(L)_2(NMe_2)_3$] (2.50 and 11, respectively), which is in agreement with a clean reaction of complex **3** with isolated surface silanols forming a single W–O–Si bond.

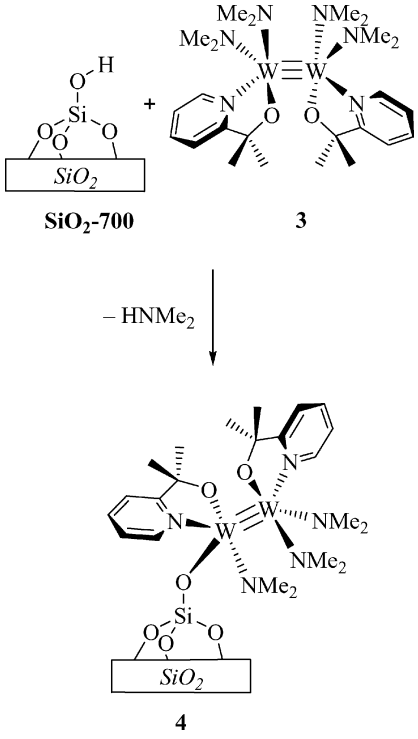

Scheme 3. Grafting of **3** onto partially dehydroxylated silica.

Diffuse reflectance infrared spectroscopic studies on **4** indicate that the silica silanol groups have been entirely consumed, as evidenced from the disappearance of the ν_{OH} signal at 3747 cm^{-1} [Figure 4, (c)]. This indicates that surface saturation has been reached during the grafting. Moreover, the spectrum of **4** comprises peaks accounting for aromatic C–H bonds (3065 and 3081 cm^{-1}) and aliphatic C–H bonds (2974–2769 cm^{-1}), as well as aromatic ring-related signals at 1607 and 1568 cm^{-1}. For these signals, the similarity with the spectroscopic features of **3** (1600 and 1567 cm^{-1}) indicates minor changes within the coordination sphere of the metal.

Solid-state NMR studies on **4** have been carried out to get a better understanding of the grafted species structure. The ^1H MAS NMR spectrum comprises peaks analogous to those observed in the ^1H solution NMR of **3** (Figure 5). Deconvolution of the spectrum is presented in Figure 6c. Aromatic protons resonate at δ = 7.2 and 9.3 ppm, the latter being assigned to C–Hs in the *ortho* position of the pyridine

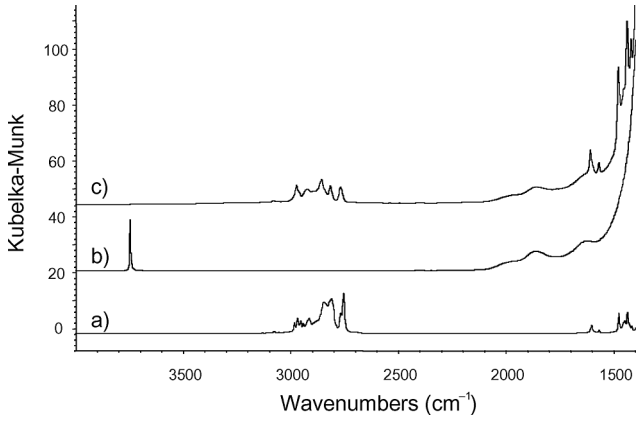

Figure 4. DRIFT spectra of a) **3**, b) SiO_2-700, c) **4**.

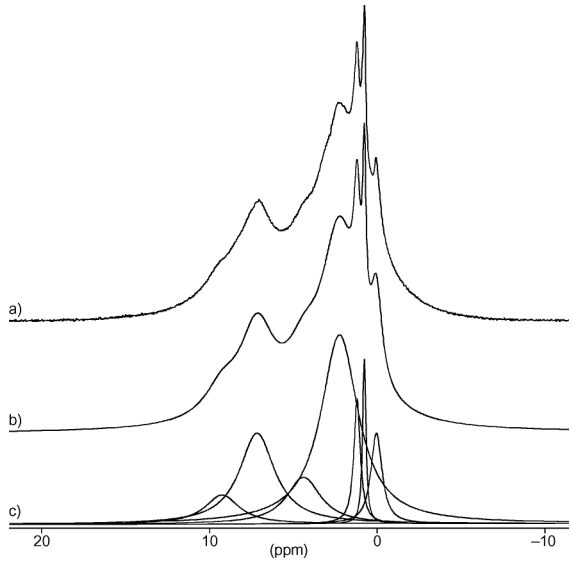

Figure 5. (a) ^1H MAS spectrum of **4** (400.1 MHz); (b) and (c) calculated spectrum and deconvolution results.

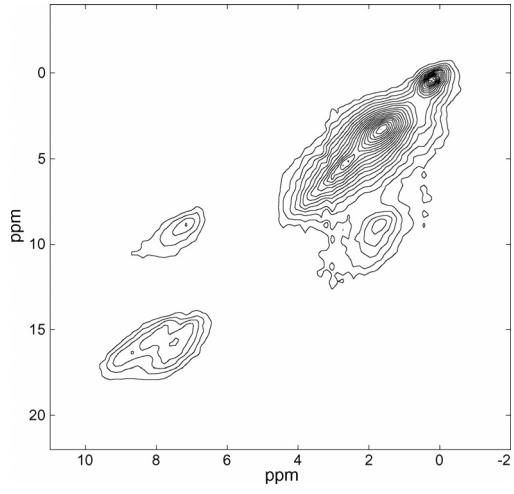

Figure 6. ^1H 2D double-quantum MAS spectrum of **4** using excitation/reconversion pulse train of one rotor period (50 μs) (800.13 MHz, 20 kHz spinning speed, pulse radio frequency 80 kHz).

fragment (C^6H). Assignment of the signals observed between 4.4 and 0.1 ppm is less straightforward. On the basis of the comparison to the signals of **3**, the peaks at δ = 4.4 and 2.3 ppm can be unambiguously assigned to NMe groups. Moreover, as a comparison, the ^{1}H MAS NMR spectrum of ≡Si–O–[$W_2(NMe_2)_5$] comprises three signals at 4.2, 3.2, and 2.5 ppm.[9] The other three signals at 1.2, 0.8, and 0.1 ppm are assigned to either NMe or diastereotopic CMe groups.[20] The high number of signals is in line with the lowering of the symmetry and increased rotation barriers due to the increased bulk resulting from the silica surface.

The use of a high-field NMR spectrometer (18.8 T, 800 MHz for ^{1}H resonance) could not significantly improve the resolution of the ^{1}H MAS NMR spectrum due to signal artifacts related to probe background signal overlapping the 0–4 ppm region. However, we have been able to run a Double Quanta MAS experiment[21] on this instrument in order to gain further insight on the structure of the grafted species of **4**. In Figure 6 is presented the spectrum resulting from the double-quantum correlation experiment using one rotor period mixing time for Back-to-Back (BABA) excitation. This technique gives the means to probe proximities between protons for which dipolar coupling is strong. Moreover, it efficiently filters out the artifacts stemming from probe background. The 2QMAS spectrum exhibits the least mobile sites that still experience sufficient dipolar coupling to correlate.

The aromatic protons give rise to two off-diagonal patterns at 9–8 ppm, assigned to the *ortho* pyridine protons based on the characteristic chemical shift, and at 8–7 ppm, for other aromatic protons. These correlations are in line with spatial proximities between these types of CHs. The broad distribution for the *ortho* pyridine protons indicates that these are present in different types of sites. This is consistent with the non-symmetric structure of the surface species and with the presence of the silica surface as a ligand, which can significantly affect the chemical shift of these nuclei in a non-homogeneous way. The other main off-diagonal interaction observed on the spectrum implies nuclei resonating around 7.3 ppm and 1.6 ppm. This corresponds to the interaction between the non-*ortho* pyridine protons and one or more CMe groups, most probably within the same [N,O] framework, an assignment in agreement with the chemical shifts of these signals. Accordingly, when comparing distances in the X-ray crystal structure (Figure 1 and Table 1), the C13-*H*–C16-*H* distance is of 2.332 Å, which is similar to the C13-*H*–C12-*H* distance (2.336 Å). Off-diagonal correlations for the NMe_2 groups are not observed on the 2D spectrum. The more rigid character of the [N,O] chelating ligand implies that the CMe_2 groups are less mobile than the NMe_2 groups, which thereby enhances the dipolar interactions, and thus increases their sensitivity to the double quantum correlation experiment compared to the dimethylamido protons. When using the two rotor periods BABA excitation, and thus probing longer interaction ranges, another off-diagonal correlation was observed between signals at 9 ppm and 1.6 ppm (Figure 7). This corresponds to *ortho* pyridine protons interacting with a C*Me* group, and, more precisely, with the same CMe which correlates with the non-*ortho* pyridine protons (this interaction is of course also visible on the spectrum). This correlation most probably implies protons located on two different [N,O] ligands on the same grafted species. Indeed, on the X-ray structure of **3**, the C10-*H*–C16^2-*H* distance is of 2.510 Å (inter-ligand interaction), much shorter than C10-*H*–C16-*H* or C10-*H*–C19-*H* distances of 5.434 and 4.730 Å, respectively (intra-ligand interaction).

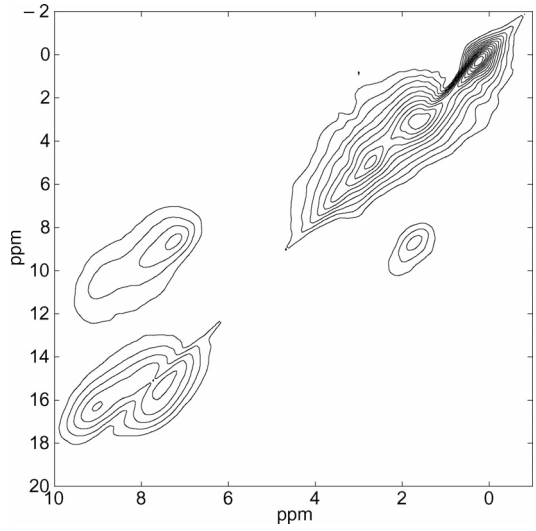

Figure 7. ^{1}H 2D double quantum MAS spectrum of **4** using excitation/reconversion pulse train of two rotor periods (100 μs) (800.13 MHz, 20 kHz spinning speed, pulse RF = 80 kHz).

^{13}C CP MAS NMR signals are reminiscent of those of the molecular precursor (Figure 8). Signals of the pyridine carbons appear at 171.8, 150.0, 135.9, and 119.3 ppm. The CMe_2 groups give rise to signals at δ = 84.1 and 81.7 ppm for two different types of *C*Me_2, and to a broad signal centered at δ = 30.5 ppm for the methyl groups. Two other peaks are observed at δ = 57.9 and 48.2 ppm, a range corresponding to WN*Me* groups. Indeed, the ^{13}C CP MAS NMR spectrum of ≡Si–O–[$W_2(NMe_2)_5$] comprises three peaks at δ = 58.2, 47.8, and 37.6 ppm.[9] Other WN*Me* signals may be hidden under the broad peak centered at δ =

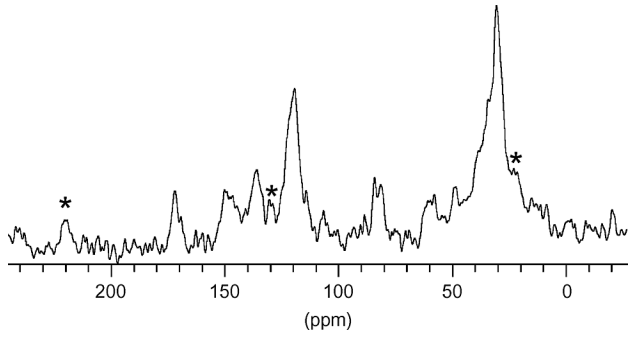

Figure 8. ^{13}C CP MAS spectrum of **4** (100.6 MHz; * denotes rotation peaks).

30.5 ppm. Again, the high number of C*Me* and N*Me* signals is consistent with the low symmetry of the grafted species.

The reactivity of **4** toward alkyne metathesis was probed. Unfortunately, this material proved to be inactive toward 4-nonyne, giving no metathesis products in detectable quantities under the conditions used for **3** (see above).

Conclusions

The synthesis of a dinuclear tungsten(III) complex bearing pyridylalkoxido and amido ligands has been accomplished through alcoholysis of the hexakis-amido ditungsten derivative. The controlled grafting of this compound has been successfully carried out, as shown by several characterization techniques. The reactivity spectrum of the molecular compound and of its grafted analogue in alkyne metathesis is narrow; only the coordination complex displays (modest) activity, under very specific conditions. The blocking of a coordination site by the pyridine nitrogen may be at the origin of the lack of reactivity of the W_2 core, by preventing access to reactive sites of the metallic species (W–N and W≡W bonds). Thus, in this case, the hemilabile character of the studied ligand may not be sufficient to perform its ascribed role, as in the case of the methoxy-substituted derivatives. Future efforts in catalyst design are in progress, aimed at introducing less coordinating functions on the alkoxide ligands.

Experimental Section

General Procedures: All experiments were performed under argon using standard Schlenk techniques or in a M-Braun glove-box, with rigorous exclusion of traces of moisture and air. THF, benzene, toluene, and hexane were purified by distillation from sodium/benzophenone ketyl and were stored over activated 4-Å molecular sieves. $[W_2(NMe_2)_6]$ was synthesized by following the literature procedure.[22] The silica support (Aerosil 380 silica, Degussa, specific area 380 $m^2 g^{-1}$) was heated under 10^{-6} mbar at 500 °C for 15 h then at 700 °C for 4 h. Elemental analyses were performed in the Service Central d'Analyses du CNRS (tungsten) and in the LSEO, University of Bourgogne (C,H,N). DRIFT spectra were recorded with a Nicolet Protégé 460 equipped with an MCT detector and a Harrick analysis chamber, with a resolution of 4 cm^{-1}. NMR liquid-phase spectra were recorded with Bruker Avance 300 and Avance 400 spectrometers at 298 K, unless specified otherwise. NMR (solid-state) spectra were recorded with a Bruker Avance 400 (^{1}H: 400.1 MHz, ^{13}C: 100.6 MHz) and Avance II 800 (^{1}H: 800.13 MHz). The ^{1}H-^{13}C CP experiments were obtained at a spinning frequency of 10 kHz, with a recycle delay of 5 s and 10240 scans were collected. For the CP step, a ramped radio-frequency (RF) field centered at 50 kHz was applied on protons, while the carbon RF field was matched to obtain an optimum signal. The contact time was set to 1.5 ms for the ^{13}C CP experiment. 2D Double Quantum Magic-Angle Spinning spectra were performed at 20 kHz spinning speed on a 18.8 T Avance II Bruker spectrometer (Larmor frequency 800.13 MHz). 2Q coherences were created using the BABA[21] scheme with mixing times of one (50 μs) or two (100 μs) rotor periods and an 80 kHz RF field. Chemical shifts for ^{1}H and ^{13}C NMR spectra are reported relative to TMS. Gas chromatography analyses were performed with a Chrompack CP9001 gas chromatograph under N_2 flow with a CPSil 8 CB column (15 m length, 0.32 mm diameter, 0.25 μm film thickness). Deconvolution was performed using the dmfit program.[23]

Synthesis of $[W_2\{(2\text{-pyr})C(Me_2)_2O\}_2(NMe_2)_4]$ (3): To a solution of $[W_2(NMe_2)_6]$ (101 mg, 0.16 mmol) in toluene (10 mL) was added a solution of 2-(2-pyridyl)propan-2-ol (260 mg, 1.9 mmol) in toluene (5 mL). The reaction mixture was stirred for 16 h at room temperature during which the solution turned deep red. All volatile compounds were removed under vacuum and the resulting red solid was heated to 60 °C under vacuum (10^{-2} mbar). The red residue was washed with a small portion of pentane where it is only slightly soluble. The product was obtained as a red powder in 40% yield. Crystals suitable for X-ray analysis were grown in pentane. $C_{24}H_{44}N_6O_2W_2$ (816.3): calcd. C 35.31, H 5.43; found C 35.27, H 5.81. ^{1}H NMR (300 MHz, [D$_6$]benzene): δ = 9.04 [dt, ^3J(H-H) = 5.4, ^4J(H-H) = 0.7 Hz, 2 H, 6-H pyr], 6.52 [dt, ^3J(H-H) = 7.6, ^4J(H-H) = 1.5 Hz, 2 H, 4-H pyr], 6.28 [ddd, ^3J(H-H) = 7.1, ^3J(H-H) = 5.6, ^4J(H-H) = 1.3 Hz, 2 H, 5-H pyr], 6.20 [dt, ^3J(H-H) = 7.8, ^4J(H-H) = 1.0 Hz, 2 H, 3-H pyr], 4.73 (s, broad, 6 H, N^1*Me*Me), 3.70 (s, 12 H, N^{2}Me$_2$), 2.28 (s, broad, 6 H, N^{1}Me*Me*), 1.75 (s, 6 H, C*Me*Me), 1.04 (s, 6 H, CMe*Me*) ppm. ^{13}C{^{1}H} NMR (100 MHz, [D$_8$]toluene, 283 K): δ = 171.60 (C-2 pyr), 150.11 (C-3 pyr), 135.38 (C-4 pyr), 121.05 (C-5, pyr), 118.26 (C-6 pyr), 80.90 (*C*Me$_2$), 57.78 (broad, NMe), 51.38 (broad, NMe), 43.23 (broad, NMe), 38.60 (C*Me*), 33.36 (C*Me*) ppm. IR [diffuse reflectance]: $\tilde{\nu}$ = 3103 (w), 3078 (w), 3055 (w), 3029 (w), 3001 (w), 2983 (m), 2969 (m), 2955 (m), 2942 (m), 2916 (m), 2846 (s), 2810 (s), 2768 (m), 2755 (s), 2708 (w), 1652 (w), 1631 (w), 1600 (w), 1567 (w), 1546 (w), 1542 (w), 1533 (w), 1475 (m), 1448 (m), 1435 (m), 1414 (w), 1395 (w), 1369 (m), 1347 (m), 1294 (m), 1273 (m), 1245 (s), 1214 (w), 1185 (s), 1155 (s), 1122 (s), 1099 (m), 1078 (m), 1053 (s), 1018 (m), 995 (s), 964 (s), 958 (s), 947 (s), 909 (w), 886 (m), 874 (w), 805 (w), 777 (s), 758 (s), 739 (w), 696 (w), 672 (w), 648 (m), 614 (s), 561 (s), 553 (m), 546 (m), 538 (m), 531 (w), 524 (m), 511 (w), 500 (w), 495 (w), 487 (w) cm^{-1}.

Synthesis of Material 4: To a suspension of SiO_2-700 (116 mg) in pentane (4 mL) was added a solution of **3** (35 mg, 43.10^{-6} mol) in pentane (4 mL). The silica rapidly turned to deep red-brown while the supernatant gradually lost its color. After overnight stirring at room temperature, the red-brown solid was separated by filtration, washed with pentane (3 × 8 mL), and dried under vacuum (10^{-6} mbar) to afford 149 mg of **4** as a deep red-brown powder. Elemental analysis (%): C 8.41, H 1.20, N 1.97, W 10.53. IR (diffuse reflectance): $\tilde{\nu}$ = 3081 (w), 3065 (w), 2974 (m), 2923 (m), 2896 (m), 2858 (m), 2816 (m), 2769 (m), 2711 (w), 1607 (m), 1568 (m), 1477 (m), 1568 (m), 1477 (s), 1419 (s), 1375 (s), 1355 (s) cm^{-1}. ^{1}H MAS (400 MHz): δ = 9.4 (sh), 7.07, 4.3, 2.07, 1.20, 0.00 ppm. ^{13}C CP-MAS (100.6 MHz): δ = 171.8, 150.0, 135.9, 130.4, 119.3, 84.1, 81.7, 57.9, 48.4, 30.5 ppm.

Catalytic Investigations: A Schlenk tube was charged with 4-nonyne (1.45 mmol), decane (0.1 mL), and toluene (5 mL), affording solution **A**, and was then heated to 363 K. A second Schlenk tube was charged with **3** (0.0254 mmol), alcohol (0.101 mmol), toluene (1 mL), and was stirred at room temperature for 10 min affording solution **B**. Solution **B** was then injected to solution **A** at 363 K. The reaction was stopped after 1 h by injection of methanol and exposition to air. Conversion and selectivity were measured by GC analysis using decane as the internal standard. Alcohols used for these tests were *tert*-butyl alcohol, 3-quinuclidinol, 1-adamandanol, and phenol.

X-ray Structural Analysis of 3: Crystal and refinement data are summarized in Table 3. X-ray data were collected with a Bruker SMART CCD area-detector diffractometer with Mo-K_α radiation (λ = 0.71073 Å) at T = 100 K. The structure was solved by direct methods.[24] Refinement against F^2 was performed by SHELX-97 with anisotropic temperature factors for non-hydrogen atoms and protons at geometrically calculated positions as riding atoms. Residuals in the final Fourier-difference map are probably due to imperfect absorption corrections.

Table 3. Crystallographic data for **3**.

Empirical formula	$C_{24}H_{44}N_6O_2W_2$
Formula mass	816.35
Crystal system	orthorhombic
Space group	*Aba*2
a [Å]	10.953(2)
b [Å]	14.556(3)
c [Å]	18.172(4)
V [Å ^{3}]	2897.3(10)
Z	4
$D_{calcd.}$ [g cm^{-3}]	1.872
μ(Mo-K_α) [mm^{-1}]	7.964
F(000)	1576
2θ range [°]	4.48–53.98
Measured reflections	10234
Unique reflections	3055
Parameters/restraints	160/1
Final *R*1	0.0250
Final *wR*2	0.0571
Goodness of fit	0.880

CCDC-652385 (for **3**) contains the supplementary crystallographic data for this paper. These data can be obtained free of charge from the Cambridge Crystallographic Data Centre via www.ccdc.cam.ac.uk/data_request/cif.

Supporting Information (see also the footnote on the first page of this article): ^{1}H NMR spectrum (room temp., C_6D_6) of intermediate $[W_2(L)(NMe_2)_5]$ obtained from the reaction of **1** with six equivalents of (L)H.

Acknowledgments

We thank the Centre National de la Recherche Scientifique (CNRS) and the Institut Universitaire de France (IUF) for their financial support and for a Ph. D. grant (to O. C.), and Bertrand Revel, Centre Commun de Mesures RMN, Université des Sciences et Technologies de Lille (USTL), for his assistance with NMR spectroscopy. Nord/Pas de Calais Region, Europe (FEDER), CNRS, French Ministry of Science, USTL and Ecole Nationale Supérieure de Chimie de Lille (ENSCL) are thanked for funding the Bruker 800 MHz spectrometer.

[1] a) A. Fürstner, P. W. Davies, *Chem. Commun.* **2005**, 2307–2320; b) A. Mortreux, O. Coutelier, *J. Mol. Catal., A* **2006**, *254*, 96–104; c) W. Zhang, J. S. Moore, *Adv. Synth. Catal.* **2007**, *349*, 93–120.
[2] R. R. Schrock, *Adv. Synth. Catal.* **2007**, *349*, 25.
[3] a) R. R. Schrock, M. L. Liestmann, L. G. Sturgeoff, *J. Am. Chem. Soc.* **1982**, *104*, 4291–4293; b) S. A. Krouse, R. R. Schrock, *Macromolecules* **1989**, *22*, 2569–2576.
[4] O. Coutelier, A. Mortreux, *Adv. Synth. Catal.* **2006**, *348*, 2038–2042.
[5] P. Braunstein, F. Naud, *Angew. Chem. Int. Ed.* **2001**, *40*, 680–699.
[6] a) O. Coutelier, G. Nowogrocki, A. Mortreux, *Abstracts of the 16th International Symposium on Olefin Metathesis and Related Chemistry*, Poznan, **2005**; b) O. Coutelier, J.-F. Paul, A. Mortreux, *Adv. Synth. Catal.*, accepted.
[7] For examples of complexes bearing bidentate pyridylalkoxido ligands, see: a) I. Kim, Y. Nishihara, R. F. Jordan, R. D. Rogers, A. L. Rheingold, G. P. A. Yap, *Organometallics* **1997**, *16*, 3314–3323; b) W. A. Herrmann, J. Fridgen, G. M. Lobmaier, M. Spiegler, *New J. Chem.* **1999**, *23*, 5–7; c) S. Bellemin-Laponnaz, K. S. Coleman, J. A. Osborn, *Polyhedron* **1999**, *18*, 2533–2536.
[8] a) M. Chabanas, A. Baudouin, C. Copéret, J.-M. Basset, *J. Am. Chem. Soc.* **2001**, *123*, 2062–2063; b) H. Weissman, K. N. Plunkett, J. S. Moore, *Angew. Chem. Int. Ed.* **2006**, *45*, 585–588.
[9] R. M. Gauvin, O. Coutelier, E. Berrier, A. Mortreux, L. Delevoye, J.-F. Paul, A.-S. Mamède, E. Payen, *Dalton Trans.* **2007**, 3127–3130.
[10] M. H. Chisholm, *Acc. Chem. Res.* **1990**, *23*, 419–425.
[11] M. H. Chisholm, *Polyhedron* **1983**, *2*, 681–722.
[12] M. Akiyama, M. H. Chisholm, F. A. Cotton, M. W. Extine, D. A. Haitko, D. Little, P. E. Fanwick, *Inorg. Chem.* **1979**, *18*, 2266–2270.
[13] J. T. Barry, J. C. Bollinger, M. H. Chisholm, K. C. Glasgow, J. C. Huffman, E. A. Lucas, E. B. Lubkovsky, W. E. Streib, *Organometallics* **1999**, *18*, 2300–2308.
[14] See for example: a) F. A. Cotton, B. R. Stults, J. M. Troup, M. H. Chisholm, M. Extine, *J. Am. Chem. Soc.* **1975**, *97*, 1242–1243; b) H. Schultz, K. Folting, J. C. Huffman, W. E. Streib, M. H. Chisholm, *Inorg. Chem.* **1993**, *32*, 6056–6066.
[15] H. Günther, *La Spectroscopie de RMN*, 5th ed., Masson, Paris, France, **1993**.
[16] M. H. Chisholm, F. A. Cotton, *Acc. Chem. Res.* **1978**, *11*, 356–362.
[17] F. J. Feher, T. A. Budzichowski, *Polyhedron* **1995**, *14*, 3239–3253.
[18] C. Copéret, M. Chabanas, R. P. Saint-Arroman, J.-M. Basset, *Angew. Chem. Int. Ed.* **2003**, *42*, 156–181.
[19] For examples of grafting of amido complexes onto inorganic supports, see: a) Q. Zhuang, K. Tanaka, M. Ichikawa, *J. Chem. Soc. Chem. Commun.* **1990**, 1477–1478; b) S. Grasser, C. Haessner, K. Koehler, F. Lefebvre, J.-M. Basset, *Phys. Chem. Chem. Phys.* **2003**, *5*, 1906–1911; c) F. Blanc, J. Thivolle-Cazat, J.-M. Basset, C. Copéret, A. S. Hock, Z. J. Tonzetich, R. R. Schrock, *J. Am. Chem. Soc.* **2007**, *129*, 1044–1045.
[20] The peak observed at δ = 0.1 ppm cannot be assigned to silicon grease, which was not used at any point in our syntheses, and for which no ^{13}C NMR signal is detected.
[21] I. Schnell, S. P. Brown, H. Y. Low, H. Ishida, H. W. Spiess, *J. Am. Chem. Soc.* **1998**, *120*, 11784–11795.
[22] M. H. Chisholm, J. D. Martin, J. E. Hill, I. P. Rothwell, *Inorg. Synth.* **1992**, *29*, 137–140.
[23] D. Massiot, F. Fayon, M. Capron, I. King, S. Le Calvé, B. Alonso, J.-O. Durand, B. Bujoli, Z. Gan, G. Hoatson, *Magn. Reson. Chem.* **2002**, *40*, 70–76.
[24] a) *SMART Software Users Guide*, version 5.0, Bruker Analytical X-ray Systems, Inc., Madison, WI, USA, **1999**; b) *SAINT Software Users Guide*, version 6.0, Bruker Analytical X-ray Systems, Inc., Madison, WI, USA, **1999**; c) G. M. Sheldrick, *SADABS*, Bruker Analytical X-ray Systems, Inc., Madison, WI, USA, **1999**; d) G. M. Sheldrick, *SHELXTL*, version 5.10, Bruker Analytical X-ray Systems, Inc., Madison, WI, USA, **1999**.

Received: July 11, 2007
Published Online: October 17, 2007

